

# Sensitivity and Selectivity of Fluorescent Chemosensor for the Detection of Fe<sup>3+</sup> and its Cell Images

Pitchai Marimuthu

Madurai Kamaraj University

Andy Ramu (✉ [andyramumku@gmail.com](mailto:andyramumku@gmail.com))

Madurai Kamaraj University

---

## Research Article

**Keywords:** Quinoline derivative, Chemosensor, Mg<sup>2+</sup> ion, ratiometric fluorescence, live-cell bio-imaging

**Posted Date:** April 28th, 2022

**DOI:** <https://doi.org/10.21203/rs.3.rs-1563804/v1>

**License:**  This work is licensed under a Creative Commons Attribution 4.0 International License.

[Read Full License](#)

---

# Abstract

A simple probe (Z)-N'-((8-hydroxyquinolin-2-yl) methylene)nicotine hydrazide (8-HQC-NH) has been synthesized and realized as a “turn-off” fluorescent chemosensor for the detection for  $\text{Fe}^{3+}$  ion over the competitive metal ions in ethanol medium. The fluorescent intensity of the 8-HQC-NH probe intensely illustrated that the “turn-off” selective quenching upon the addition of  $\text{Fe}^{3+}$  owing to the chelation-enhanced fluorescence quenching (CHEQ) effect. The probe of 8-HQC-NH exhibited an ample linear response towards  $\text{Fe}^{3+}$  concentration ranging between 0 to 75  $\mu\text{M}$  with satisfactory lower detection limits of  $7 \times 10^{-8}$  M. Furthermore, the developed 8-HQC-NH probe offers many advantages like good biocompatibility, negligible cytotoxicity, being promising efficient fluorescent probe to recognize  $\text{Fe}^{3+}$  ions in living cells. These features explore the way for the design of simple and efficient fluorescent method for the bio-sensing applications.

## Introduction

The rapid and selective sensing of iron(III) metal ions ( $\text{Fe}^{3+}$ ) is extensively fascinated owing to the ubiquitous existence of Fe in the ecological and biological systems [1]. Several metal ions play important roles in biological systems and contamination of metal ions constitutes an obvious hazard toward the environmental system. However, the dishomeostasis of  $\text{Fe}^{3+}$  ion is hazardous to humans in severe health disarrays such as skin syndromes, insomnia, and immunity deterioration [2]. Furthermore, the environmental issues are becoming worsened with inorganic pollutants like  $\text{Fe}^{3+}$  ions due to the prompt expansion of industries [3]. Hence, the detection of  $\text{Fe}^{3+}$  ions with high selectivity and sensitivity is a crucial task [4]. Despite the diverse techniques that have been reported in the literature including UV-Vis spectroscopy, atomic absorption spectroscopy (AAS) [5], chromatographic [6], potentiometric [7], chemoluminescence [8] and the polarography detection utilized to detect the  $\text{Fe}^{3+}$  ions, but however, requires complex systems and expensive instruments [9–11]. Therefore, development of easily synthesisable probe for the simple and low cost techniques for the detection of  $\text{Fe}^{3+}$  ion is highly desirable process [12].

The spectrofluorometric chemosensors employing fluorescent probe is a most versatile technique for the determination of metal ions including  $\text{Fe}^{3+}$  owing to the affordable cost [13], ease operation techniques, high sensitivity, prompt response, and easy scrutinizing of target ions [14–17]. Despite substantial results of fluorescence chemosensors towards the recognition of  $\text{Fe}^{3+}$ , the selective fluorescent probes are still remained sporadic owing to their paramagnetic characteristics of  $\text{Fe}^{3+}$  ion [18] and less solubility nature of organic fluorescent probes in aqueous solutions [19–22]. Since, the fluorescence responses are rely on numerous mechanisms [23], the design and development of cost-effective [24], highly selective, and sensitive fluorogenic probes for the detection of  $\text{Fe}^{3+}$  ions is still challenging [25–28]. In a current advancement, the photosensitive chemosensors are depended on diverse sensing mechanisms including, photo-induced electron transfer (PET), metal-ligand charge transfer (CT), chelation enhanced fluorescence (CHEF) [29], intramolecular charge transfer (ICT) [30], fluorescence resonance energy transfer (FRET) [31], and excited-state intramolecular proton transfer (EIPT) [32].

Amid the CHEQ based sensor exists impel in the competent research field appealing owing to the chemosensor from the above deliberations [33], Schiff bases derivatives including strong fluorophores from the simple synthetic steps are the appropriate aspirant toward the sensing of  $\text{Fe}^{3+}$  ions [34]. Hence, the present work reports the fluorescent turn-off chemosensor for the  $\text{Fe}^{3+}$  ion detection with quinoline-based probe (8-HQC-NH), which is facilely obtained through a readily synthesizable Schiff base reaction between imine from 8-hydroxyquinoline-2-carboxaldehyde and nicotinohydrazide. The probe was characterized by ESI-MS and NMR techniques. The fluorescence experiments of selected metal ions showed a dramatic fluorescence intensity enhancement for  $\text{Fe}^{3+}$  respect to other cations. This exhibited that 8-HQC-NH is a deserved probe to sense  $\text{Fe}^{3+}$  ion and this binding mechanism of 8-HQC-NH with  $\text{Fe}^{3+}$  ions was also studied using theoretical studies and the observed results are discussed appropriately.

## Determination Of The Limit Of Detection And Binding Constant

The limit of detection was calculated using the formula,  $3\sigma/s$ , where  $\sigma$  is the standard deviation of blank solution and slope ( $s$ ) is derived by the calibration curve. The binding constant was determined from the fluorescence data employing reformed Benesi-Hildebrand Eq. 1.

$$1/\Delta I = 1/\Delta I_{\max} + (1/K [C]) (1/\Delta I_{\max}). \text{ Here } \Delta I = I - I_{\min} \text{ and } \Delta I_{\max} = I_{\max} - I_{\min} \text{ (Eq. 1)}$$

where  $I_{\min}$ ,  $I$ ,  $I_{\max}$  are the emission intensities of the probe in the absence of  $\text{Fe}^{3+}$  ion, at an intermediate  $\text{Fe}^{3+}$  concentration, and at a concentration of complete saturation where  $K$  is the binding constant and  $[C]$  is the  $\text{Fe}^{3+}$  concentration respectively. The binding constant  $k$  calculated from the plot of  $(I_{\max} - I_{\min}) / (I - I_{\min})$  against  $[C]^{-1}$  of  $\text{Fe}^{3+}$  ion [36–37].

## 2.2. Stock solution preparation

For the preparation of the stock solution,  $1 \times 10^{-3}$  M concentration was maintained as standard for 8-HQC-NH and the metal ion solutions in DMSO and double distilled water, respectively. A 25  $\mu\text{M}$  of 8-HQC-NH was prepared through the dilution of 50  $\mu\text{L}$  of 8-HQC-NH ( $1 \times 10^{-3}$  M) solution into the 2 mL of DMSO and kept the same concentrations for all the fluorescence analysis [35].

## 2.3. Synthesis of (Z)-N'-((8-hydroxyquinolin-2-yl) methylene) nicotinohydrazide (8-HQC-NH)

Synthesis of 8-HQC-NH was prepared as described briefly here. A 1 mmol of nicotinohydrazide (0.042g) was added to 20 ml of ethanol solution containing 8-hydroxyquinoline-2-carbaldehyde (0.01 g, 1 mmol) and this solution was refluxed at 85  $^{\circ}\text{C}$  for 4h. The completion of the reaction was monitored by thin layer chromatography and after completion of the reaction, the reactions mixture was cooled down to room temperature. The organic layer was washed twice with 10 mL of distilled water and then dried over anhydrous sodium sulfate. Later, this crude mixture was further purified by column chromatography

(ethyl acetate: Pet ether). Finally, a yellow solid was obtained with 80% yield and the reaction is shown in Scheme 1.

## 2.4 Instrumentation

The UV-Vis spectra were recorded on a JASCO-500 spectrophotometer with a quartz cuvette (cell length 1cm). The fluorescence spectra were recorded with an Agilent Cary Eclipse Fluorescence Spectrofluorimeter.  $^1\text{H}$  and  $^{13}\text{C}$  NMR spectra were recorded on a BRUKER 300 MHz spectrometer using  $\text{CDCl}_3$  and  $\text{DMSO-d}_6$  as solvent and using TMS as the internal standard. ESI-MS analysis was performed on the positive and negative ion modes on a liquid chromatography–ion-trap mass spectrometry instrument (LCQ Fleet, Thermo Fisher Instruments Limited, USA). DFT calculations were performed at the B3LYP/LANL2DZ (d) level using the Gaussian 09 program. This labour all reagents and solvents were used as received from commercial suppliers without further purification.

## Results And Discussion

The quinoline based chemosensor 8-HQC-NH was synthesized as depicted in Scheme 1. In line with the research interests of our group to cultivate various probes for the development of new sensors and catalytic applications, we designed a novel quinoline based probe 8-HQC-NH using 8-hydroxyquinoline-2-carbaldehyde through the condensation of nicotinohydrazide in ethanol. The as-synthesised probe, 8-HQC-NH is characterized by  $^1\text{H}$ ,  $^{13}\text{C}$ -NMR and ESI-MS analyses and the observed data are shown in Figures S1-S2. Briefly, the structural aspects of this probe exactly matches with NMR and the mass value of the probe also verified by ESI-MS. Thus, these analytical data confirm the purity of the probe and no other impurities are present.

### 3.1. UV-Vis studies of 8-HQC-NH

The UV-Vis absorption spectrum is measured for the as-prepared probe with various metal ions and the observed data are shown in Fig. 1a. The probe (50  $\mu\text{M}$ ) exhibits an absorption band at 292 nm in aqueous solution owing to the  $\pi\text{-}\pi^*$  transition. The addition of  $\text{Fe}^{3+}$  ion to the solution decreases the intensity of a predominant UV-Vis band of the probe (292 nm) and produce new absorption band at 340 nm, detailing the occurrence of the strong coordination between the probe and  $\text{Fe}^{3+}$  ion. The negligible change in the UV-Vis spectrum is observed for the probe after the addition of other metal ions even in the presence of  $\text{Fe}^{3+}$  ion. Furthermore, the intensity of a band in the UV-Vis spectra are gradually increased upon increasing the concentration of  $\text{Fe}^{3+}$  ions in the range between 0–90  $\mu\text{M}$  (Fig. 1b), specifying the formation of the stable coordination complex.

### 3.2. Fluorescence spectral studies of 8-HQC-NH

The selectivity of the 8-HQC-NH probe has been investigated through the fluorescence studies with the interfering species including  $\text{Al}^{3+}$ ,  $\text{Cu}^{2+}$ ,  $\text{Cr}^{3+}$ ,  $\text{Zn}^{2+}$ ,  $\text{Hg}^{2+}$ ,  $\text{Mg}^{2+}$ ,  $\text{Ni}^{2+}$ ,  $\text{Cd}^{2+}$ ,  $\text{Mn}^{2+}$ ,  $\text{Co}^{2+}$ , and  $\text{Fe}^{3+}$  at a concentration of 25  $\mu\text{M}$ . The acquired fluorescence spectra reveal that the extensive fluorescence

quenching at 430 nm and a negligible effect is observed with Fe<sup>3+</sup> ions and the other metal ions, respectively [Figure 2a]. This result shows that the 8-HQC-NH has respectable selectivity towards Fe<sup>3+</sup> ion over the other competing cations, elucidating strong interaction between the functional groups of 8-HQC-NH and Fe<sup>3+</sup> ions. The fluorescence spectra of 8-HQC-NH were recorded at an excitation wavelength of 340 nm with a diverse concentration of Fe<sup>3+</sup> (Fig. 2b), which exhibits a gradual decrement with the increased concentration of Fe<sup>3+</sup> ions (0–70 μM). Furthermore, the quenching efficiency is analyzed by following Stern-Volmer Eq. 2

$$\text{Eq.: } F_0/F = K_{sv} [Q] + 1 \dots\dots\dots (\text{Eq. 2})$$

Where  $F_0$  and  $F$  are the intensities of 8-HQC-NH before and after addition of Fe<sup>3+</sup>,  $[Q]$  is the molar concentration of the Fe<sup>3+</sup> and  $K_{sv}$  is the quenching constant. The working curve is mapped by  $(F_0 - F)/F_0$  of 8-HQC-NH with the concentration of Fe<sup>3+</sup> and exhibits a good linear correlation ( $R^2 = 0.9876$ ) in a concentration ranging from 0–70 μM were show in (Fig. 3a). From the concentration analysis, the detection limits of the probe toward the sensing of Fe<sup>3+</sup> ions was estimated to be  $7.0 \times 10^{-8}$  M, which is inferior and comparable to those of reported sensors[38–42]. The binding constant of 8-HQC-NH with Fe<sup>3+</sup> was found to be  $3.6 \times 10^{-3} \text{ M}^{-1}$  using the fluorescence titration data (Fig. 3b). The competitive experiments of 8-HQC-NH toward Fe<sup>3+</sup> ion were evaluated with an ample range of co-existing metal ions including Al<sup>3+</sup>, Cu<sup>2+</sup>, Cr<sup>2+</sup>, Zn<sup>2+</sup>, Hg<sup>2+</sup>, Mg<sup>2+</sup>, Ni<sup>2+</sup>, Cd<sup>2+</sup>, Mn<sup>2+</sup> and Co<sup>2+</sup> at a concentration of 25 μM and the resulting fluorescence spectra are illustrated in (Fig. 4). The competitive metal ions fluorescence spectra do not influence any significant quenching in the Fe<sup>3+</sup> ion spectra and observed identical fluorescence responses with the co-existing metal ions, which reveals the high selectivity of the probe towards the sensing of Fe<sup>3+</sup> ions. Further, the job's plot analysis also confirmed the interaction between 8-HQC-NH is ratio 1:1 (Fig. 5). This binding stoichiometric was further confirmed by ESI-MS data as shown in Figure S2. When Fe<sup>3+</sup> ion is added to the probe, a complex is formed with the assistance of anchoring sites including hydroxyl of quinoline ring, nitrogen of hydrazide moiety. Due to this complexation, the chelation-enhanced fluorescence quenching (CHEQ) is suppressed. The proposed sensing of 8-HQC-NH under the present experimental conditions in the present system is based on CHEQ mechanism. This mechanism takes place from the electron-rich quinoline to hydrazide and the whole process is shown in Scheme 2. This indicates that only with 8-HQC-NH, strongly binds with Fe<sup>3+</sup> ion through the formation of coordination complex has occurred. Similarly, the intensity of the band was decreased and that of the band at 433 nm is quenched, due to the formation complex between 8-HQC-NH and Fe<sup>3+</sup> ions. This result indicates a more efficient coordination of Fe<sup>3+</sup> ion occurs with the hydroxyl of quinoline ring, the nitrogen of quinoline moiety, imine nitrogen (C = N) and the nitrogen of hydrazide moiety. Upon addition of Fe<sup>3+</sup> ion, the charge transfer was arrested due to the strong complexation of Fe<sup>3+</sup> with 8-HQC-NH. In addition, it is well known that Fe<sup>3+</sup> ion (a soft acid), especially interacts with the nitrogen, and hydroxyl group according to Pearson's HSAB theory, thus supporting the observed data with this probe for the selective detection of Fe<sup>3+</sup> ion.

## Theoretical Studies With Confocal Cell Imaging

The geometry of 8-HQC-NH was optimized using DFT-B3LYP/6-31G level using Gaussian 09 packages. The chemosensor 8-HQC-NH is the best platform to form a strong complex with  $\text{Fe}^{3+}$  in 1:1 stoichiometric manner and this stoichiometric complex was supported by Job's plot analysis. DFT calculations are an excellent tool for elucidating the sensing mechanism of the chemosensor. It shows that the chemosensor has band gap value between the HOMO and LUMO is 2.28 eV and after complex formation, this energy gap is decreased to 1.04 eV, this reveals the strong binding nature of the chemosensor with  $\text{Fe}^{3+}$  ions. In addition, the electrons are lies on quinoline moiety in HOMO and LUMO shows electron density over all the chemosensor. Moreover, the 8-HQC-NH- $\text{Fe}^{3+}$  complex shows more electron density on metal centre at HOMO and LUMO, thus indicating the strong chelation of chemosensor with  $\text{Fe}^{3+}$  ions and the complex may be formed at ground state. The metal unbound state chemosensor shows strong fluorescence which is attributed to the quinoline moiety and due to more paramagnetic nature of the  $\text{Fe}^{3+}$  ions forms a complex with chemosensor to enhance CHEQ leading to the fluorescence quenching(Fig. 6).

The fluorescence imaging experiments were performed to evaluate the sensitivity of chemosensor 8-HQC-NH to sense  $\text{Fe}^{3+}$  in HeLa cells. The HeLa cells were hatched with 5  $\mu\text{M}$  of chemosensor in DMSO/PBS buffer (pH 7, 1/49, v/v) at 36°C for 40 min and imaged through laser scanning confocal fluorescence microscopy at 340 nm excitation (Fig. 7). Initially, HeLa cells were incubated with 5  $\mu\text{M}$  8-HQC-NH for 5 h and it shows strong green fluorescence image. The observed fluorescent color imaging significantly diminished in the presence of 25  $\mu\text{M}$  of  $\text{Fe}^{3+}$  ion, which elucidates that the 8-HQC-NH probe can be suitable for the efficient detection of  $\text{Fe}^{3+}$  ion in biological systems.

Table 1

Comparison table for the detection of Fe<sup>3+</sup> with various probes reported in the literature.

S. No.	Probe	Metal ion	Detection limit	Application	Ref.
1	Pyridine-pyrazole	Fe <sup>3+</sup>	6.1 x 10 <sup>2</sup> M <sup>-1</sup>	Fluorescent "turn-off" sensor	38
2	3-formyl-9H-hexylcarbazole	Fe <sup>3+</sup>	2.57 x 10 <sup>-4</sup> M	Fluorescent "turn-on" sensor	39
3	2-hydroxy-1-naphthaldehyde and 2-aminopyridine	Fe <sup>3+</sup> Zn <sup>2+</sup>	2.0 x 10 <sup>-5</sup> M 5.0 x 10 <sup>-6</sup> M	Fluorescent "turn-on" sensor	40
4	6-thiophen-2-yl-5,6-dihydro-benzo[4,5]imidazo[1,2-c]quinazoline	Fe <sup>3+</sup>	3.88 x 10 <sup>-5</sup> M	Fluorescent "turn-on" sensor	41
5	2-(N-methylpiperazinylimino)acetaldehyde	Fe <sup>3+</sup>	6.9 x 10 <sup>-3</sup> M	Fluorescent "turn-on" sensor	42
6	8-HQC-NH	Fe <sup>3+</sup>	7.0 x 10 <sup>-8</sup> M	"Turn-off" and Live cell imaging	This work

## Conclusions

In conclusion, this work has designed a simple and readily synthesisable Schiff base of 8-HQC-NH as a probe for sensing of Fe<sup>3+</sup> ions and showed as chemosensors with higher selectivity and sensitivity over the diverse competitive metal ions. The chemosensor probe was characterized by <sup>1</sup>H, <sup>13</sup>C-NMR and ESI-MS spectroscopic techniques. The sensing mechanism of this quenched chemosensor was explained by using DFT analysis which shows that the probe expresses clear CHEQ mechanism and later, the addition of the Fe<sup>3+</sup> ions indicates the suppression of CHEQ quenching was seen at 433 nm. Moreover, fluorescence imaging testing of 8-HQC-NH in HeLa cells clearly demonstrated that the biocompatible and low cytotoxicity of this probe provides an effective approach to the selective detection of Fe<sup>3+</sup> ions in biological samples. Thus, some of the salient features of this method are bio-compatibility, rapid response and high selectivity of Fe<sup>3+</sup> ions in the presence of other competing metal ions. Therefore, the reported sensor is expected to expand demand in a sensor field as well as in the development of medical kits.

# Declarations

## Acknowledgements:

P. M. extending his acknowledgement to School of Chemistry, Madurai Kamaraj University for providing adequate instrument facilities through DST-IRHPA, FIST, DST-PURSE and UGC-UPE schemes.

## Authors' Contributions:

All authors contributed in the present study. All authors commented on this version of the manuscript and they read and approved the final manuscript.

## Funding:

The authors have no relevant financial or non-financial interests to disclose.

## Data Availability:

All data contained in the current manuscript and supplementary information are available.

**Conflict of interest:** All authors declare no conflict of interest.

**Ethics approval:** Not applicable.

**Consent to participate:** Not applicable.

**Consent to publish:** Not applicable.

## Supplementary information:

The complementary information about all experiments and theoretical calculations is included in the supplementary information.

# References

1. F. Yan, T. Zheng, Y. Zou, Y. Wang, L. Chen, Rhodamine amino pyridine based fluorescent sensors for  $\text{Fe}^{3+}$  in water Synthesis, quantum chemical interpretation and living cell application, *Sens Actuators B Chem.* 215 (2015) 598-606.
2. A. S. Murugan, E.R. A. Noelson, J. Annaraj, Solvent dependent colorimetric, ratiometric dual sensor for copper and fluoride ions: Real sample analysis, cytotoxicity and computational studies, *Inorganica Chimica Acta.* 450 (2016) 131–139.
3. L. Jin, C. Liu, Q. Zhang, J. Wang, L.Y. Zhao, Fluorescence turn-on detection of  $\text{Fe}^{3+}$  in pure water based on a cationic poly (perylene dimide) derivative, *RSC Adv.* 6 (2016) 58394-58400.

4. A. Luo, H. Wang, Y. Wang, Q. Huang, Q. Zhang, A novel colorimetric and turn-on fluorescent chemosensor for iron (III) ion detection and its application to cellular imaging, *Spectrochimica Acta Part A: Molecular and Biomolecular Spectroscopy*. 168 (2016) 37-44.
5. Y.W. Choi, G.J. Park, H.Y. Jo, S.A. Lee, G.R. You, C. Kim, A single Schiff base molecule for recognizing multiple metal ions: A fluorescence sensor for Zn(II) and Al(III) and colorimetric sensor for Fe(II) and Fe(III), *Sens Actuators B Chem.* 194 (2014) 343-352.
6. F. He. Wang, C. W. Cheng, L. C. Duan, W. Lei, M. Z. Xia, F. Y. Wang. Highly selective fluorescent sensor for Hg<sup>2+</sup> ion based on a novel rhodamine B derivative, *Sensors and Actuators B Chem.* 206 (2015) 679-683.
7. Z.Q. Hu, Y.C. Feng, H.Q. Huang, L. Ding, X.M. Wang, C.S. Lin, M. Li, C. P. Ma, Fe<sup>3+</sup> selective fluorescent probe based on rhodamine and its application in bioimaging, *Sens Actuators B Chem.* 156 (2011) 428-432.
8. P. Suresh, I. A. Azath, K. Pitchumani, Naked-eye detection of Fe<sup>3+</sup> and Ru<sup>3+</sup> in water: Colorimetric and ratiometric sensor based on per-6-amino-β-cyclodextrin/p-nitrophenol, *Sens Actuators B Chem.* 146 (2010) 273-277.
9. S. Devaraj, Y.K. Tsui, C.Y. Chiang, Y.P. Yen, A new dual functional sensor: Highly selective colorimetric chemosensor for Fe<sup>3+</sup> and fluorescent sensor for Mg<sup>2+</sup>, *Spectrochimica Acta Part A: Molecular and Biomolecular Spectroscopy*. 96 (2012) 594-599.
10. S. N. swamy, T. Govindaraju, Aldazine-based colorimetric sensors for Cu<sup>2+</sup> and Fe<sup>3+</sup>, *Sens. Actuators B Chem.* 161 (2012) 304-310.
11. Y. T. Liang, G. P. Yang, B. Liu, Y. T. Yan, Z. P. Xi, Y. Y. Wang, Four super water-stable lanthanide-organic frameworks with active uncoordinated carboxylic and pyridyl groups for selective luminescence sensing of Fe<sup>3+</sup>, *Dalton Trans.*, 2015, 44, 13325-13330.
12. G. Sivaraman, V. Sathiyaraja, D. Chellappa, Turn-on fluorogenic and chromogenic detection of Fe(III) and its application in living cell imaging, *J. Lumin.* 145 (2014) 480-485.
13. Y. Shiraishi, S. Sumiya, Y. Kohno, T. Hirai, A rhodamine-cyclen conjugate as a highly sensitive and selective fluorescent chemosensor for Hg(II), *J. Org. Chem.* 73 (2008) 8571-8574.
14. M. Yang, M. Sun, Z. Zhang, S. Wang, A novel dansyl-based fluorescent probe for highly selective detection of ferric ions, *Talanta*. 105 (2013) 34-39.
15. S. Dalapati, S. Jana, Md.A. Alam, N. Guchhait. Multifunctional fluorescent probe selective for Cu(II) and Fe(III) with dual-mode of binding approach. *Sens Actuators B* 160 (2011) 1106-1111.
16. G. Men, C. Chen, S. Zhang, C. Liang, Y. Wang, M. Deng, H. Shang, B. Yang, S. Jiang, A real-time fluorescent sensor specific to Mg<sup>2+</sup> crystallographic evidence, DFT calculation and its use for quantitative determination of magnesium in drinking water, *Dalton Trans.* 44 (2015) 2755-2762.
17. D. En, Y. Guo, B. Chen, B. Dong, M. Peng, Coumarin-derived Fe<sup>3+</sup> selective fluorescent turn-off chemosensors synthesis, properties, and applications in living cells, *RSC Adv*, 4 (2014) 248-253.

18. S. Adewuyi, D. A. Ondigo, R. Zuggle, Z. Tshentu, T. Nyokong, N. Torto, A highly Selective and sensitive pyridylazo-2-naphthol-poly(acrylic acid) functionalized electrospun nano-fiber fluorescence "turn-off" chemosensory system for Ni<sup>2+</sup>, *Anal. Methods*. 4 (2012) 1729-1735.
19. Z. Chen, Y. Sun, L. Zhang, D. Sun, F. Liu, Q. Meng, R. Wang, D. Sun, A tubular europium-organic framework exhibiting selective sensing of Fe<sup>3+</sup> and Al<sup>3+</sup> over mixed metal ions, *Chem. Commun.* 49 (2013) 11557-11559.
20. M.D. Yang, Y. Zhang, W.J. Zhu, H.Z. Wang, J. Huang, L.H. Cheng, H.P. Zhou, J. Y. Wu and Y.P. Tian, Difunctional chemosensor for Cu(II) and Zn(II) based on Schiff base modified anthryl derivative with aggregation-induced emission enhancement and piezochromic characteristics, *J. Mater. Chem.* **3** (2015) 1994-2002.
21. M. Zheng, H. Tan, Z. Xie, L. Zhang, X. Jing, Z. Sun, Fast response and high sensitivity europium metal organic framework fluorescent probe with chelating terpyridine sites for Fe<sup>3+</sup> fast response and high sensitivity europium metal organic framework fluorescent probe with chelating terpyridine sites for Fe<sup>3+</sup>, *ACS Appl. Mater. Interface.* 5 (2013) 1078-1083.
22. A.J. Weerasinghe, F.A. Abebe, E. Sinn, Rhodamine based turn-ON dual sensor for Fe<sup>3+</sup> and Cu<sup>2+</sup>, *Tetrahedron Letters* 52 (2011) 5648-5651.
23. P. Li, M. Zhang, X. Sun, S. Guan, G. Zhang, M. Baumgarten, K. Müllen, Adendrimer-based highly sensitive and selective fluorescence-quenching sensor for Fe<sup>3+</sup> both in solution and as film, *Biosens. Bioelectron.* 85 (2016) 785-791.
24. S.P. Wu, Y.P. Chen, Y.M. Sung, Colorimetric detection of Fe<sup>3+</sup> ions using pyrophosphate functionalized gold nanoparticles, *Analyst* 136 (2011) 1887-1891.
25. T.B. Wei, P. Zhang, B.B. Shi, P.C. Qi, L.J. Liu, Y.M. Zhang, A highly selective chemosensor for colorimetric detection of Fe<sup>3+</sup> and fluorescence turn-on response of Zn<sup>2+</sup>, *Dyes Pigments* 97 (2013) 297-302.
26. S. Wang, X. Meng, M. Zhu, A naked-eye rhodamine-based fluorescent probe for Fe(III) and its application in living cells, *Tetrahedron Letters.* 52 (2011) 2840-2843.
27. S.K. Shoor, A.K. Jain, V.K. Gupta, A simple Schiff base based novel optical probe for aluminium (III) ions, *Sens. Actuators B Chem.* 216 (2015) 86-10.
28. M. Kumar, R. Kumar, V. Bhalla, P.R. Sharma, T. Kaur, Y. Qurishi, Thiocalix[4]arene based fluorescent probe for sensing and imaging of Fe<sup>3+</sup> ions, *Dalton Transactions.* 41 (2012) 408-412.
29. Y.H. He, J.P. Lai, H. Sun, Z.M. Chen, S. Lan, A fast, sensitive and stable fluorescent fiber-optic chemosensor for quantitative detection of Fe<sup>3+</sup> in real water and HepG2 living cells, *Sens. Actuators B Chem.* 225 (2016) 405-412.
30. Z. Hu, Y. Feng, H. Huang, L. Ding, X. Wang, C. Lin, M. Li, C. Ma, Fe<sup>3+</sup> selective fluorescent probe based on rhodamine B and its application in bioimaging, *Sens. Actuators B Chem.* 156 (2011) 428-432.
31. M.H. Lee, T.V. Giap, S.H. Kim, Y.H. Lee, C. Kang, J.S. Kim, A novel strategy to selectively detect Fe(III) in aqueous media driven by hydrolysis of a rhodamine 6G Schiff base, *Chem. Commun.* 46 (2010)

1407-1409.

32. D. Zhang, M. Li, M. Wang, J. Wang, X. Yang, Y. Ye, Y. Zhao, A rhodaminephosphonate off-on fluorescent sensor for  $\text{Hg}^{2+}$  in natural water and its application in live cell imaging, *Sens. Actuators B-Chem.* 177 (2013) 997-1002.
33. G. Sivaraman, T. Anand, D. Chellappa, Development of a pyrene based 'turn on' fluorescent chemosensor for  $\text{Hg}^{2+}$ , *RSC Adv.* 2 (2012) 10605-10609.
34. L. Rao, Y. Tang, Z. Li, X. Ding, G. Liang, H. Lu, C. Yan, K. Tang, B. Yu, Efficient synthesis of highly fluorescent carbon dots by micro reactor method and their application in  $\text{Fe}^{3+}$  ion detection, *Mater. Sci. Eng.C-Mater. Bio. Appl.* 81 (2017) 213–223.
35. H.A. Benesi, J.H. Hildebrand, A spectrophotometric investigation of the interaction of iodine with aromatic hydrocarbons, *Journal of the American Chemical Society.* 71 (1949) 2703-2707.
36. Y. C. Liao, P. Venkatesan, L. F. Wei, S. P. Wu, A coumarin-based fluorescent probe for thiols and its application in cell imaging, *Sens. Actuators B Chem.* 232 (2016) 732-737.
37. S. R. Liu, S. P. Wu, New water-soluble highly selective fluorescent chemosensor for Fe (III) ions and its application to living cell imaging, *Sensors and Actuators B Chem.* 171 (2012) 1110-1116.
38. Y. R. Bhorge, H. T. Tsai, K. F. Huang, A.J. Pape, S. N. Janaki, Y. P. Yen, A new pyrene-based Schiff-base: A selective colorimetric and fluorescent chemosensor for detection of Cu(II) and Fe(III), *Spectrochim. Acta Part A Mol. Biomol. Spectrosc.* 130 (2014) 7-12.
39. R. Kumar, P. Gahlyan, N. Yadav, M. Bhandari, R. Kakkar, M. Dalela, A.K. Prasad, Bistriazolylated-1,4-dihydropyridine highly selective hydrophilic fluorescent probe for detection of  $\text{Fe}^{3+}$ , *Dyes Pigments.* 147 (2017) 420-428.
40. R.K. Pathak, J. Dessingou, V.K. Hinge, A.G. Thawari, S.K. Basu, C.P. Rao, Quinoline driven fluorescence turn on 1,3-bis-calix[4]arene conjugate-based receptor to discriminate  $\text{Fe}^{3+}$  from  $\text{Fe}^{2+}$ , *Anal. Chem.* 85 (2013) 3707-3714.
41. S. Elçin, H. Deligöz, A.A. Bhatti, M. Oguz, S. Karakurt, M. Yilmaz, Synthesis and evaluation of fluorescence properties of  $\text{Cu}^{2+}$  selective azocalix[4]arenes and their application in living cell imaging, *Sens. Actuators B Chem.* 234 (2016) 345-352.
42. J. Zhang, L. Zhao, Y. Liu, M. Li, G. Li, X. Meng, Two luminescent transition-metal-organic frameworks with predesigned ligand as highly sensitive and selective iron(III) sensors, *New J. Chem.* 00 (2018) 1-3.

## Scheme

Scheme 1-2 are available in Supplementary Files section.

## Figures

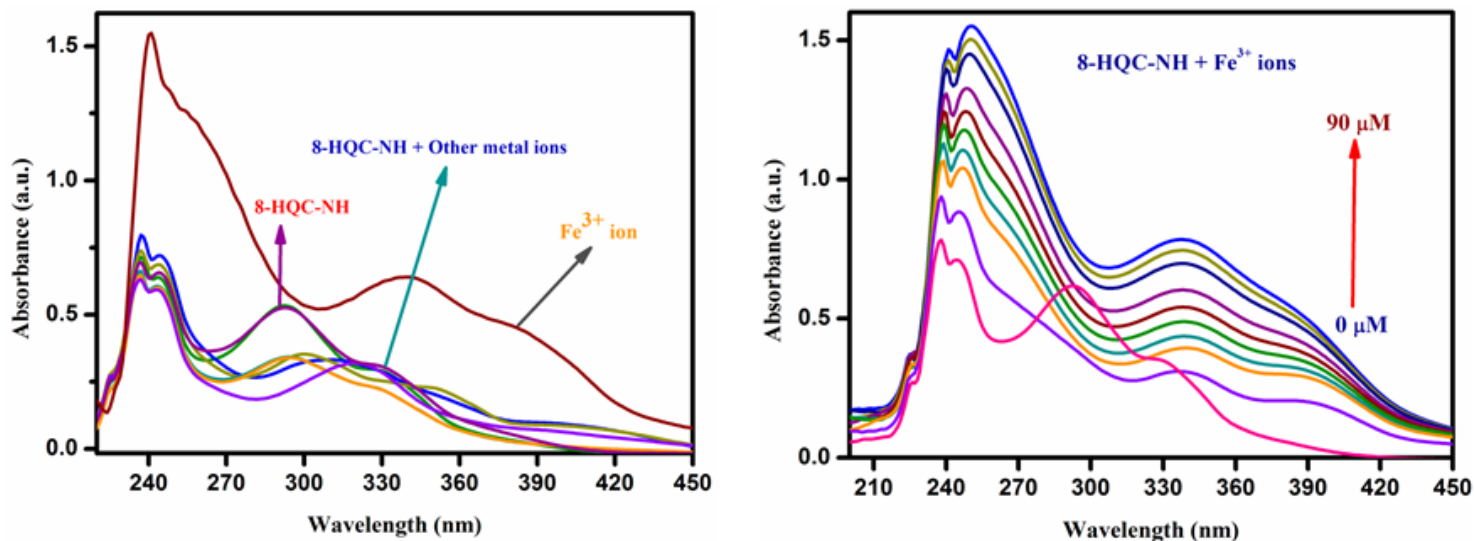


**Figure 1**

a) UV-Visible spectra of 8-HQC-NH (25  $\mu\text{M}$ ) in the presence of various metal ions such as  $\text{Al}^{3+}$ ,  $\text{Cu}^{2+}$ ,  $\text{Cr}^{3+}$ ,  $\text{Zn}^{2+}$ ,  $\text{Hg}^{2+}$ ,  $\text{Mg}^{2+}$ ,  $\text{Ni}^{2+}$ ,  $\text{Cd}^{2+}$ ,  $\text{Mn}^{2+}$ ,  $\text{Co}^{2+}$ , and  $\text{Fe}^{3+}$  (25  $\mu\text{M}$ ) in ethanol. b) UV-Visible spectra of 8-HQC-NH (25  $\mu\text{M}$ ) upon the titration with  $\text{Fe}^{3+}$  (0 to 90 mM) in ethanol.

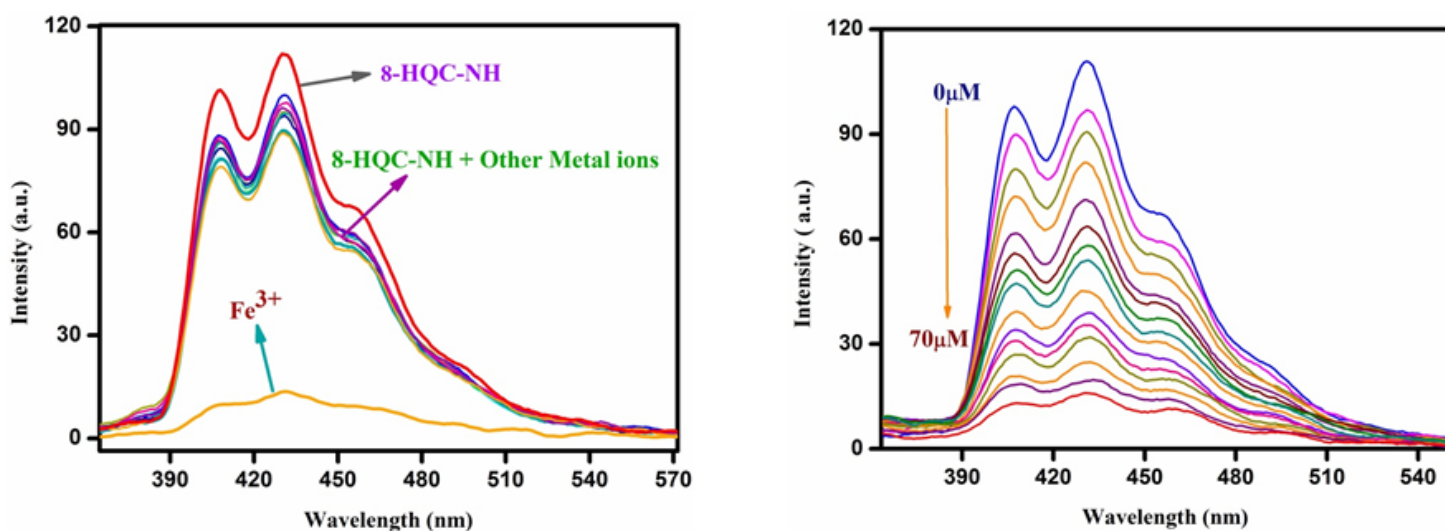


**Figure 2**

a) Fluorescence spectra of 8-HQC-NH (25  $\mu\text{M}$ ) in the presence of various metal ions such as  $\text{Al}^{3+}$ ,  $\text{Cu}^{2+}$ ,  $\text{Cr}^{3+}$ ,  $\text{Zn}^{2+}$ ,  $\text{Hg}^{2+}$ ,  $\text{Mg}^{2+}$ ,  $\text{Ni}^{2+}$ ,  $\text{Cd}^{2+}$ ,  $\text{Mn}^{2+}$ ,  $\text{Co}^{2+}$ , and  $\text{Fe}^{3+}$  (25  $\mu\text{M}$ ) in ethanol. b) Fluorescence spectra of 8-HQC-NH (25  $\mu\text{M}$ ) upon the titration of  $\text{Fe}^{3+}$  (0 to 70 mM) in ethanol.

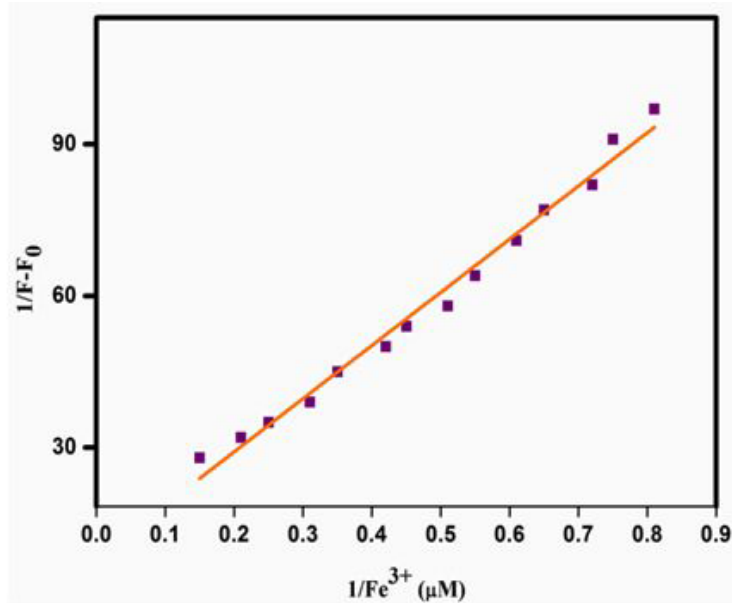
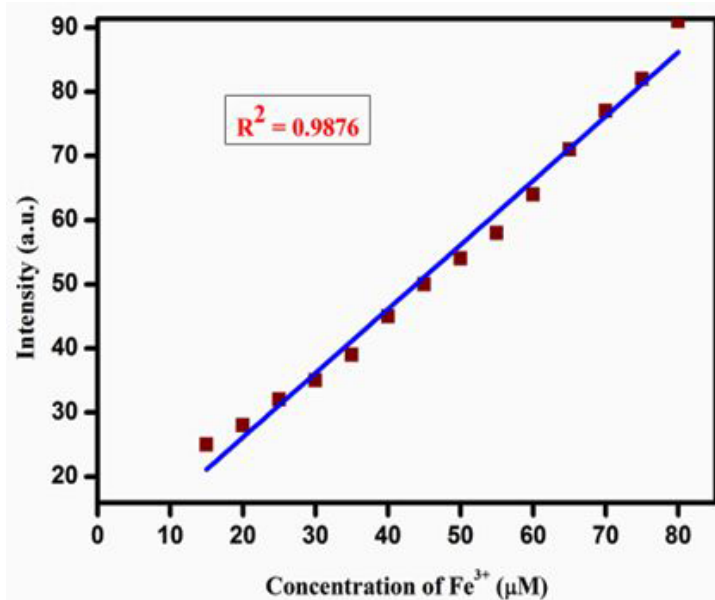


Figure 3

a) Linear relationship plot obtained from fluorescence titration of 8-HQC-NH (μM) with a concentration of Fe<sup>3+</sup> ions (0 to 70mM). b) Benesi-Hildebrand plot, determination of the Binding constant for a probe with Fe<sup>3+</sup> ion.

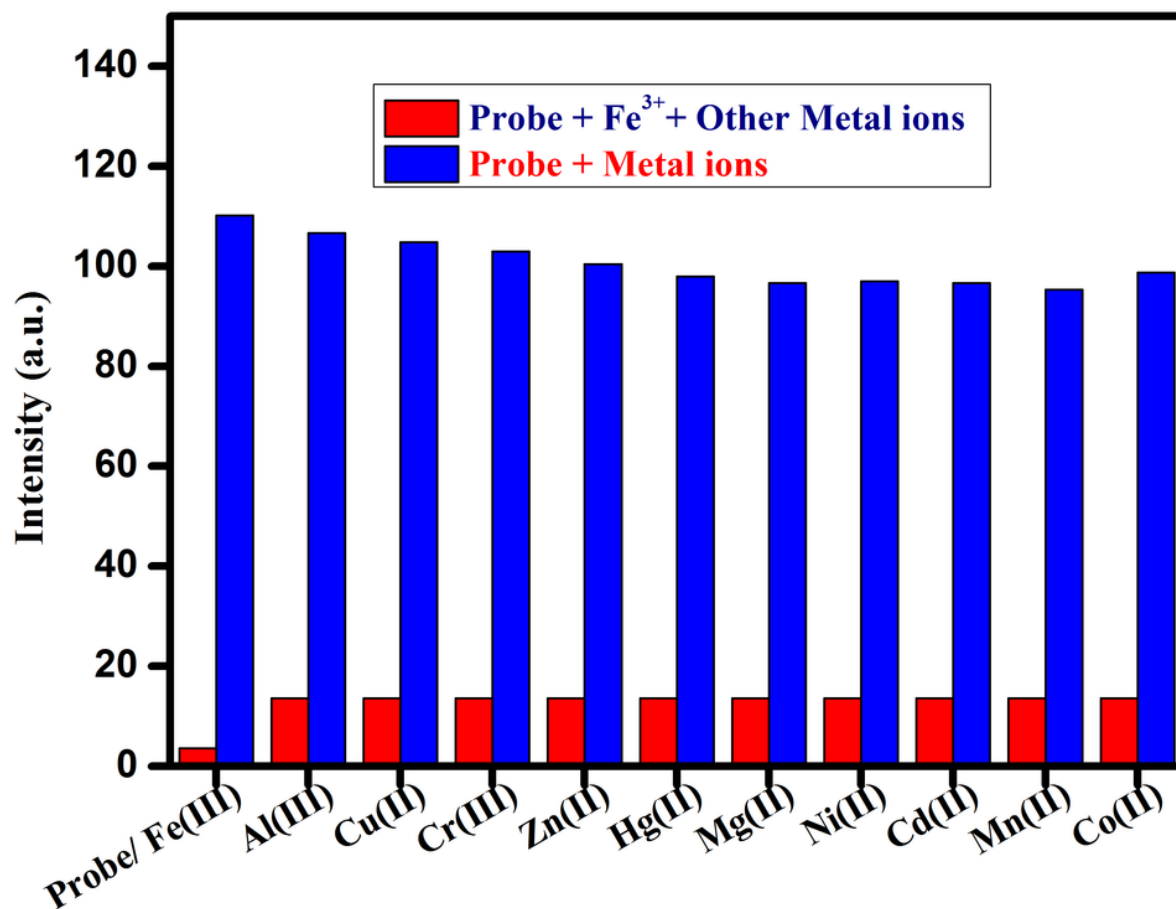


Figure 4

Competitive experiments of 8- HQC-NH toward Fe<sup>3+</sup>: red bars represent of various metal ions with an added into an 8- HQC-NH + Fe<sup>3+</sup> in ethanol solution and blue bars represent fluorescence intensity of 8- HQC-NH + Metal ions,  $\lambda_{ex}$  340nm. (25  $\mu$ M),

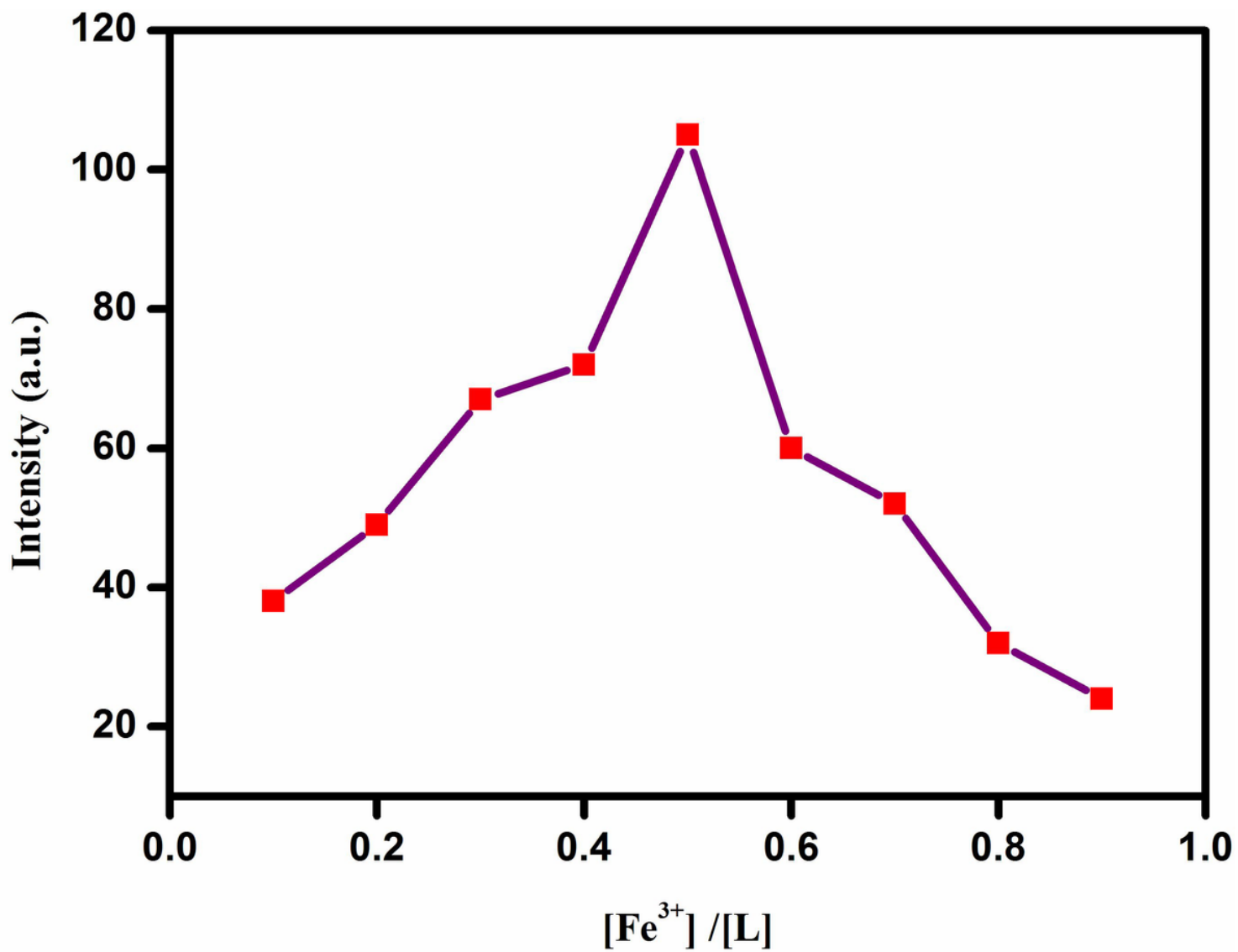
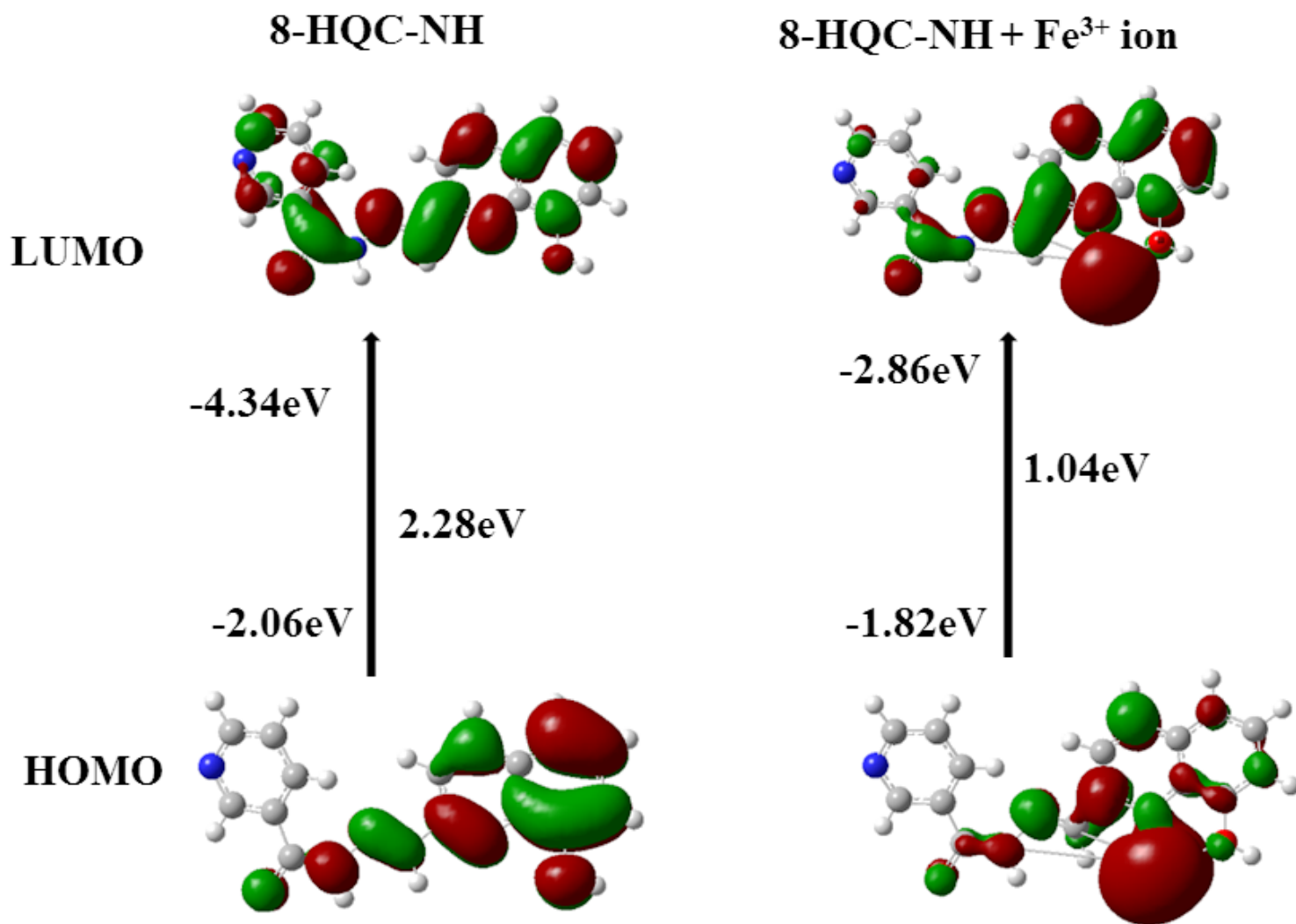


Figure 5

Job's diagram between 8- HQC-NH and  $Fe^{3+}$  ion.



**Figure 6**

HOMO and LUMO of (Z)-N'-((8-hydroxyquinolin-2-yl) methylene) nicotinohydrazide (8-HQC-NH) calculated with DFT/TD-DFT at B3LYP/6-31G (d) level using Gaussian 09.

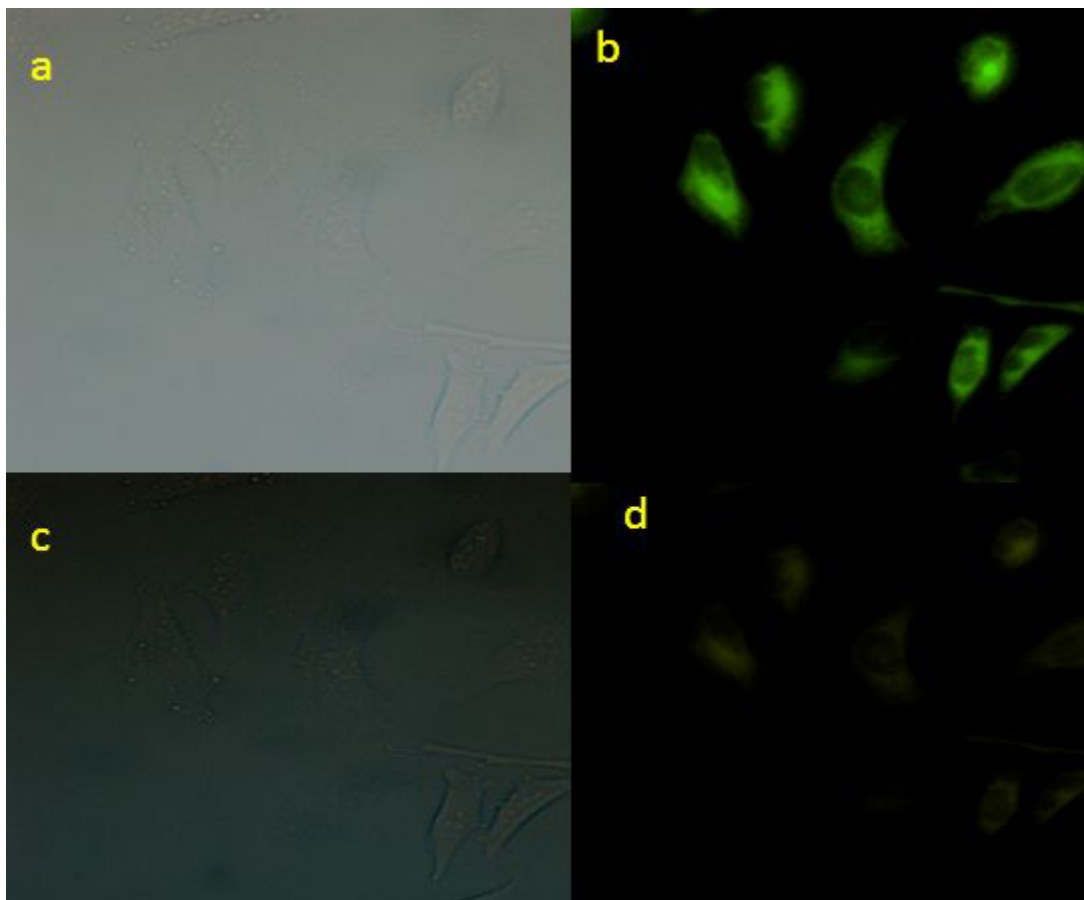


**Figure 7**

Bright field image of (a) 8-HQC-NH and (b) 8-HQC-NH with  $\text{Fe}^{3+}$  ions, fluorescence images of 8-HQC-NH and (c) 8-HQC-NH with  $\text{Fe}^{3+}$  ions (d) Overlay image of 8-HQC-NH and 8-HQC-NH with  $\text{Fe}^{3+}$  ions in Ethanol/PBS buffer (pH7, 1/49, v/v) at  $36^\circ\text{C}$  for 40 min.

## Supplementary Files

This is a list of supplementary files associated with this preprint. Click to download.

- [RevisedSupplemetaryFile.doc](#)
- [GraphicalAbstract.jpg](#)
- [Highlights.doc](#)
- [scheme1.png](#)
- [scheme2.png](#)